

FATIGUE AND DAMAGE TOLERANCE TESTING OF GRIPEN E/F RUDDER

Jan Erik Lindbäck¹, Zlatan Kapidžić¹, Allan Gustavsson¹ and Risto Laakso²

¹ Saab AB, jan-erik.lindback@saabgroup.com

² VTT Technical Research Centre of Finland Ltd.

Abstract: A structural test of Gripen 39E/F rudder was performed to verify the safe-life and damage tolerance of the rudder structure. Two different design load sequences, one representing the operational profile of 39E-version and the other for the 39F-version, with the latter being more severe, have been considered. Preliminary analyses have shown that a test using the more severe sequence 39F would likely not be able to verify the full service life. Therefore, a strategy was adopted to test the 39E sequence with upscaled loads during a part of the test campaign and thereby verify the 39E sequence, as well as part of the service life of 39F. The test was successfully run to a number of simulated flight hours where the most critical crack had grown from an artificial defect to a predicted critical length. A subsequent static test showed that the structure had sufficient residual strength. This paper presents an analytical procedure, based on fatigue and crack growth calculations, to determine the corresponding percentage of 39F service life that is considered to be verified by the performed test. This approach shows a cost-efficient way to utilize the test results as much as possible, without jeopardizing the primary goal of validating the configuration 39E of the aircraft.

Keywords: Fatigue, Damage Tolerance, Test, Rudder

INTRODUCTION

Generally, the structural integrity assessment program for the Gripen 39E/F aircraft follows the procedures and specifications according to MIL-STD-1530C and JSSG-2006 to ensure service life and damage tolerance (DT) [1]. Structural parts of the airframe and systems are designed for safe-life with a remotely low probability of fatigue crack initiation, 10^{-4} , at full service life. Additionally, all safety-of-flight structural parts are categorized as fracture critical and are subject to DT assessment for the purpose of ensuring the flight safety of the aircraft. The critical parts shall be capable of maintaining adequate residual strength in presence of material, manufacturing and processing defects until the damage is detected through inspections. The DT assessment assumes that such defects are present at the most stressed points in the critical parts from the beginning of the life of the aircraft.

In addition to the safe-life and DT design, the service life and DT capability needs to be verified by full-scale structural testing. The remotely low probability of fatigue crack initiation is normally verified by fatigue testing for 4 design life (DL), whereafter the test object should not contain any significant fatigue damage. The verifying DT test is first run for 2 DL to ensure subcritical, slow crack growth from

artificially manufactured defects in critical parts. Thereafter, a static test is performed to verify that the residual structural strength has not been degraded below 120% of limit load (LL).

Compared to the previous versions of the Gripen aircraft, the 39E/F versions have undergone significant structural design changes and are designed for new operational profiles. This led to a rather extensive verifying test program [1], including full-scale static and fatigue tests, and fatigue and DT tests of assemblies and control surfaces, among them the rudder. The rudder was fatigue and DT tested at VTT's test facility in Espoo as a part of the certification process of the Gripen 39E/F aircraft. Gripen 39E (referred to as 39E hereafter), see Figure 1, is a single-seater and Gripen 39F (referred to as 39F hereafter) is a two-seater but some structural parts, for instance the rudder, are identical. The operational profiles differ between the two and 39F is subjected to a more severe design load spectrum than 39E. This paper describes the testing and analysis approach to verify the safe-life and DT of both the 39E and 39F rudder with the same structural test object.



Figure 1: Gripen 39E with the rudder highlighted with a red dotted line. Copyright SAAB AB, photo Linus Svensson.

The rudder design is a sandwich honeycomb with bonded aluminium skins on each side. There are three hinge lugs and one actuating jack lug at the interface to the fin, see Figure 2. The yellow-colored parts in Figure 2 are categorized as critical parts. The verifying test program consists of a combined fatigue and DT test, where the whole rudder structure is verified for safe-life, while the critical parts are also verified for DT by introduction of artificial defects during the test campaign.

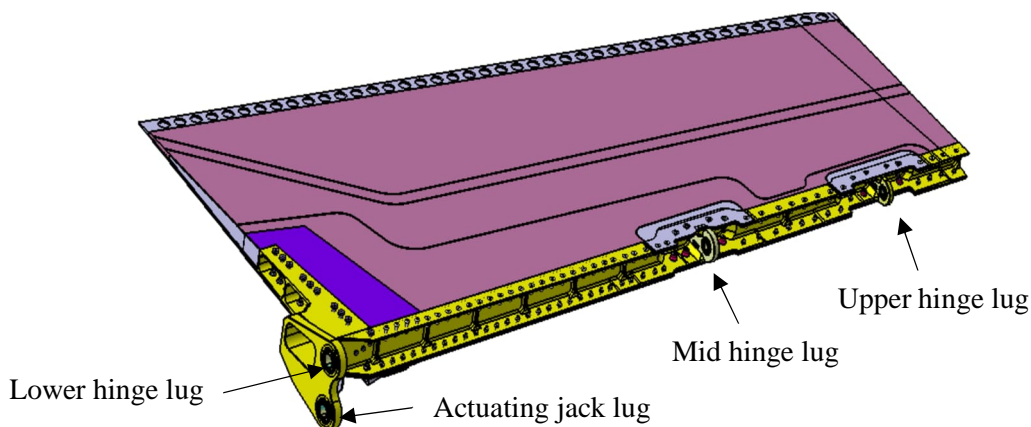


Figure 2: The overall rudder design with critical parts shown in yellow.

Verification testing strategy for Gripen 39E/F rudder

The 39F design load sequence is more severe than the 39E load sequence. Based on preliminary analyses, it was found that the rudder probably would not sustain verifying testing corresponding to one full service life for the 39F load sequence. A number of options were considered regarding the fatigue and DT test strategy:

- To run the more severe 39F sequence and risk to break the rudder, or have a too fast crack growth

- To run two separate test objects, one to verify the 39E-sequence and one for 39F-sequence
- To first run the 39E-sequence followed by a residual strength test and then run the 39F-sequence
- To first run the 39E-sequence followed by a residual strength test and then continue with the same load sequence but upscaled. After the completion of the test, determine the number of verified flight hours for 39F by analysis.

The first two options were dismissed due to risk, cost and schedule reasons. The third option was turned down for two reasons. First for simplicity, to avoid having to deal with two different sequences and second to avoid crack growth rate retardation effects. The last option was preferred, mainly to avoid jeopardizing the verification of the 39E rudder. The 39E rudder is considered to be fatigue and DT verified after 4 DL of fatigue loading, of which the last two also have artificial defects, followed by a residual strength test (RST) to 120% LL for some selected critical load cases. Maximum envelope spectrum loads are close to the max envelope LL. A sequence load scaling with a factor of 1.2 was proposed after 4 DL, i.e. the same magnitude as for the residual strength test. This approach was chosen to avoid retardation effect caused by the residual strength test. The second part of the test, with the purpose to cover 39F, was aimed for another 2 DL with spectrum loads scaled with a factor of 1.2, followed by another RST to 144% LL. This approach was considered as severe for the rudder structure and frequent crack growth inspections were therefore performed to lower the risk of failure before or during the residual strength test to 144% LL.

Provided that the first part of the test to verify 39E was successful, there was still a challenging analysis to perform to show that also 39F can be covered. The approach was to test as many cycles as possible up to the final 144% RST and thereafter determine the corresponding number of equivalent 39F flight hours by analysis. The test result together with the analysis will then show whether 39F will be fully verified or if additional inspections or a rudder replacement have to be considered.

TESTING

The rudder test at VTT Technical Research Centre of Finland Ltd (VTT) and Eurofins Expert Services Ltd (EES) took approximately eight months from October 2021 to mid-May 2022, of which fatigue and DT testing with non-destructive inspections 3.5 months [2]. The introduction of artificial defects at Saab with rudder shipments back and forth, including the Christmas break, took ten weeks in lead time. The following sections describe, in some detail, the test object, rig, loads, test procedure and test results.

Test object

The test object, shown in Figure 2, was a rudder identical to a flying part. Prior to the test, initial fatigue and DT analyses of the rudder structure were performed and five points were identified as potentially fatigue critical. Those five points are the locations where the artificial defects were introduced in the test object after 2DL of testing, see Figure 3.

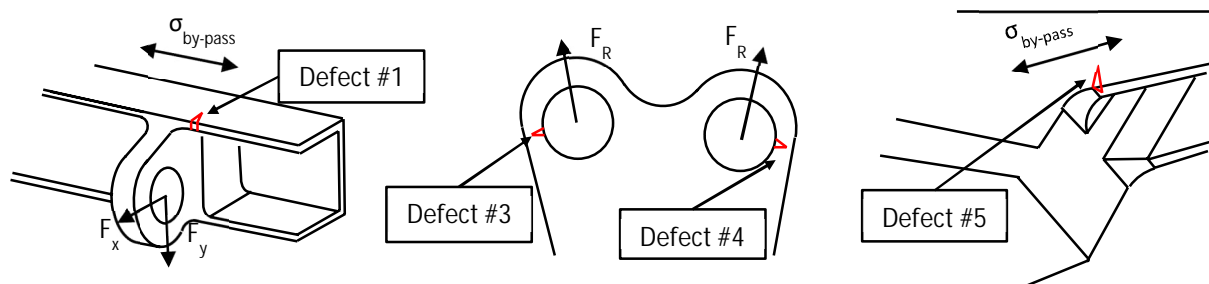


Figure 3: Left: Single edge corner defect #1 at the upper hinge. A similar defect at the mid hinge is called defect #2. Mid: Lug corner defect #3 at the actuator jack lug and defect #4 at the lower hinge lug. Right: Single edge corner defect #5 at lower fitting radius.

Electro-spark machining is a preferred defect manufacturing method, because it minimizes the risk of introducing plastic deformations, however it was infeasible due to the size and complexity of the test object. Instead, the defects were manufactured by saw-cutting using the tool set-up shown in Figure 4.

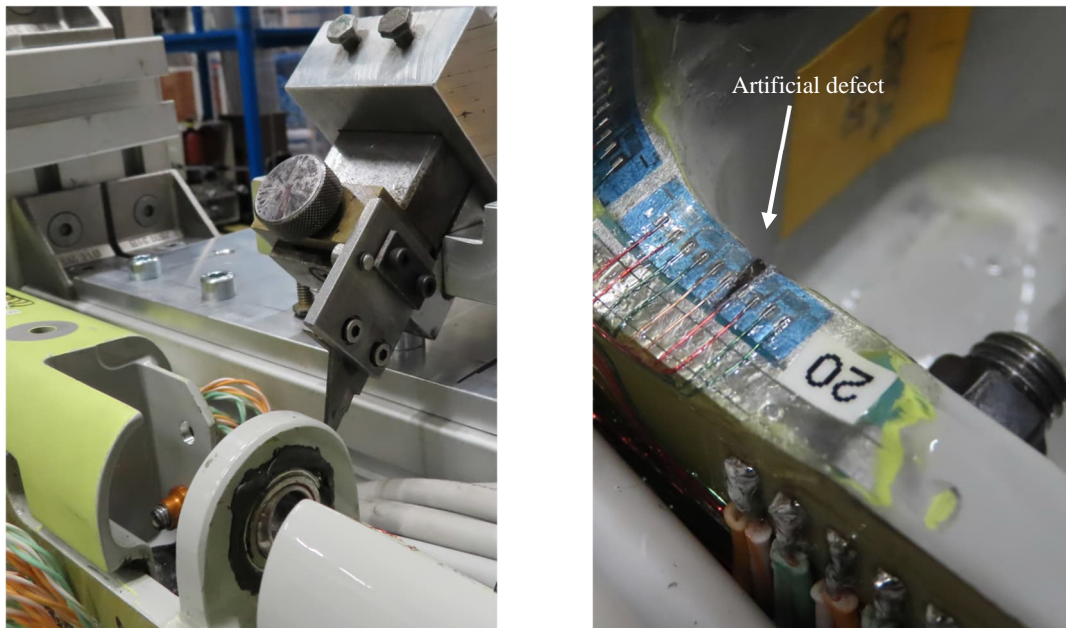


Figure 4: Left: Saw-cut tool set up at defect #2 at the mid hinge. Right: Detail of defect #2 interferred with a row of strain gauges.

Test rig

The rudder test set-up was constructed and erected to VTT's Research Hall, at the EES R-hall test floor with associated infrastructure. The tests were performed in normal laboratory conditions. The rig contained the actuators as a floating and free-standing unit and all actuators were integrated in the rig itself, see Figure 5.

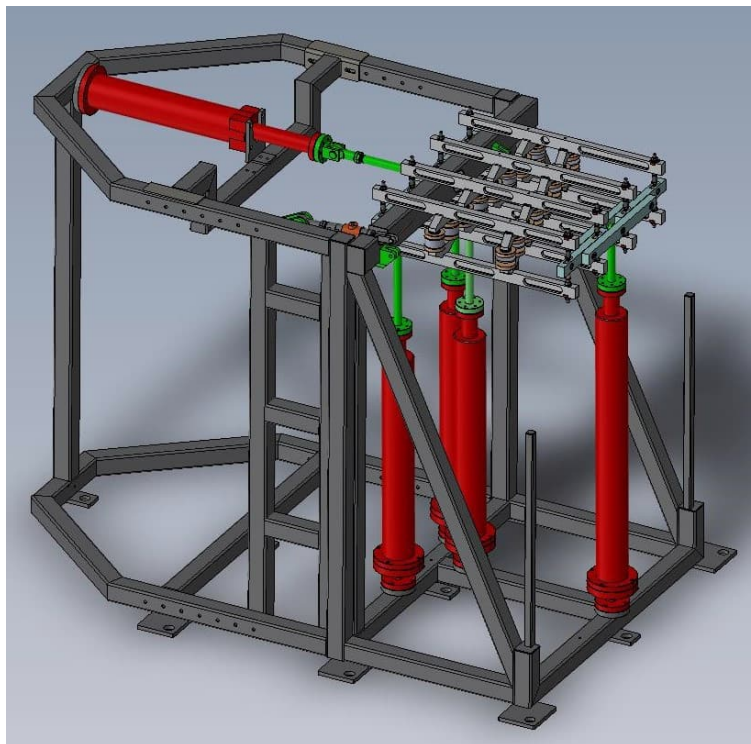


Figure 5: Test set-up before rudder mounting. Figure courtesy of Arecap Ltd, A. Mattila.

The same test set-up was used for all test stages. The design work of the test set-up structures was an iterative process, which was done in very close cooperation with Saab, VTT, EES, and Arecap Ltd. Arecap prepared the drawings and manufactured the rig with loading structures, see Figure 6.



Figure 6: Test rig and loading structures. Figure courtesy of EES, J. Juntunen.

A whiffle-tree structure with 32 pads and 5 actuators were used to introduce the load to the test object, see Figure 6. The in-flight air loads were applied with three actuators (denoted C1, C2 and C3) to the whiffle-tree, while two other actuators (C4 and C5) simulated the correct reaction loads on the middle hinge of the rudder. Upper and lower hinges of the rudder were constrained in x- and y-directions, perpendicular to the hinge line, similar to the aircraft conditions. The rudder jack operates the rudder in flight but was constrained in the test to carry the rudder moment and the reaction load was instrumented with a load cell. The tests did not represent any high-frequency buffeting in terms of high frequency loading. No master cylinders were used, thus all five actuators were managed independently. All tests were controlled by a load control mode, where the feedback transducer signal was taken from the actuator load cell. Feedback from an additional accelerometer was used to stabilize the control system. The weight of the assembly and the rudder were compensated for by a tare procedure [3].

Test loads

Figure 7 shows the FE-model of the test object and the load application arrangement with the whiffle-tree system, pads and actuator loads. The actuator test load sequences were determined, using the FE-model, so that the correct hinge and rudder jack loads are obtained.

A large number of low-range load cycles were eliminated from the test spectrum to reduce the testing time. The reduced 39E load spectrum had about 450 000 load turning points for one DL. Three 39E residual strength load cases were selected. They covered the highest crack-opening load for all five cracks. One of these load cases, downscaled to 80% LL, was run several times during the test campaign. The purpose was to collect the data from strain gauges, displacement transducers and the load cell in order to identify any deviations over time that may be caused by crack growth. This load case is called the static reference case.

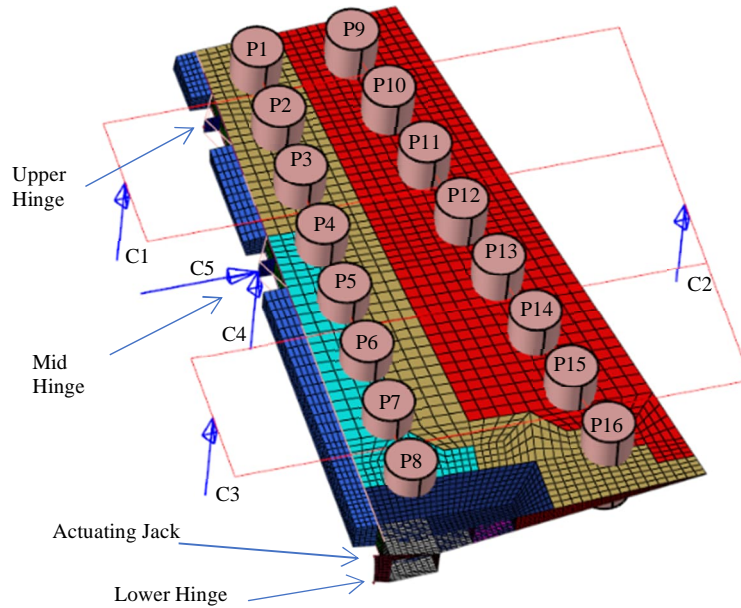


Figure 7: FE-model of the rudder with pad and whiffle tree structure illustrated.

Test procedure

The test duration was about 75 hours wall clock time for one DL. When applying scaled-up loads, the load introducing speed was slowed down 20% to make sure that the system was well stabilized. The test duration of 1 DL increased to around 96 hours wall clock time. Static, fatigue and DT tests, as well as RST, and non-destructive inspection (NDI) followed the test plan. A brief overview is shown in Table 1.

Table 1: Test procedure.

<i>Test phase</i>	<i>Accumulated test time</i>	<i>Actions</i>
Fatigue testing	1 DL	Static and dynamic set-up tests, tare loads, dynamic calibrations, static tests, run up to 0.5 design life, static ref test, run up to 1 design life, static ref test and NDI.
	2 DL	Run up to 1.5 lives, static ref test, run up to 2 lives, static ref test and NDI.
Introduction of artificial defects	2 DL	The rudder was shipped to Saab where five artificial defects were introduced.
Fatigue and DT testing	2.5 DL	Static ref test, run up to 2.5 lives, static ref test and NDI.
	3 DL	Run up to 3 lives, static ref test and NDI.
	3.5 DL	Static ref test, run up to 3.5 lives, static ref test and NDI.
	4 DL	Run up to 4 lives, static ref test, NDI, RST 120% LL and NDI.
Additional fatigue and DT testing at 120%	4.5 DL	Static ref test, run up to 4.5 lives, static ref test and NDI.
	5 DL	Run up to 5 lives, static ref test and NDI.
	5.5 DL	Run up to 5.25 lives, static ref test and NDI, run up to 5.5 lives, static ref test and NDI.
	5.75 DL	Run up to 5.75 lives, static ref test and NDI.
Events after 5.75 DL	5.75 DL	RST 144 % LL and NDI, dismounting and final tear down NDI.

All test variables: support reactions, actuator loads and displacements, and rudder's displacements and strains were monitored and stored as time histories in all test phases. A total of 132 quarter-bridge strain gauge channels were used. Non-destructive inspections were performed at basically the same intervals as the planned static reference tests. Survey data was recorded separately and checked to see if there were any major differences compared to previous recordings. Measurement of the crack lengths was performed during the static reference tests. Non-destructive testing was done with eddy current testing and ultrasonic inspections as well as with frequent visual inspections and liquid penetrant. All inspection levels and areas were described in more detail in [4]. Only some levels were inspections without dismounting the rudder from the test rig. Dismounting provided considerably better accessibility and was even mandatory in some areas.

Test results

Instrumentation data, from strain gauges, displacement transducers and the load cell, were extracted for every static reference load case occasion. The results were compared with the previous occasion to identify deviations that could indicate a load redistribution caused by a structural defect. No or very small deviations were found between the different occasions, which indicated an overall strength integrity of the rudder throughout the test campaign. Measured far field strains agreed acceptably well with predicted strains computed by the FE model, which was one purpose of the test to verify.

A row of single strain gauges located close to the artificial defect #3, with the purpose to identify any local load redistribution in case of crack growth, indicated a slight load alleviation when comparing the RST after 5.75 DL with RST after 4 DL. This observation agrees well with the identified crack growth.

NDI was performed on several occasions, see Table 1. The copper wiring of the strain gauges, close to the artificial cracks, disturbed the NDI performed with eddy current technology. Additional liquid penetrant testing was therefore also used at some occasions. It was also difficult to have access to the fatigue critical areas with the rudder mounted in the rig. Therefore, the rudder was dismounted from the rig and inspected on a table after 4 DL and after completed testing at 5.75 DL. To measure the point #3 crack length was found difficult and the accuracy may be questioned which is also further discussed below.

In all, the tests followed the test plan. All rig and loading structures as well as equipment worked successfully. No fatigue findings were identified during the test campaign. No crack growth was found after 4 DL followed by RST which verified the 39E aircraft.

Crack growth was first observed at defect #3 during the 1.2x39E sequence load between 4.5 and 5 DL. There was also minor crack growth from other defects, but this paper will only focus on the most critical defect #3. The artificial defect introduced at 2 DL was measured to 1.4 mm. The fatigue crack that grew from defect #3 is shown, after 5.75 DL, in Figure 8. The test was stopped at 5.75 DL, when the crack length was close to the calculated critical crack length.

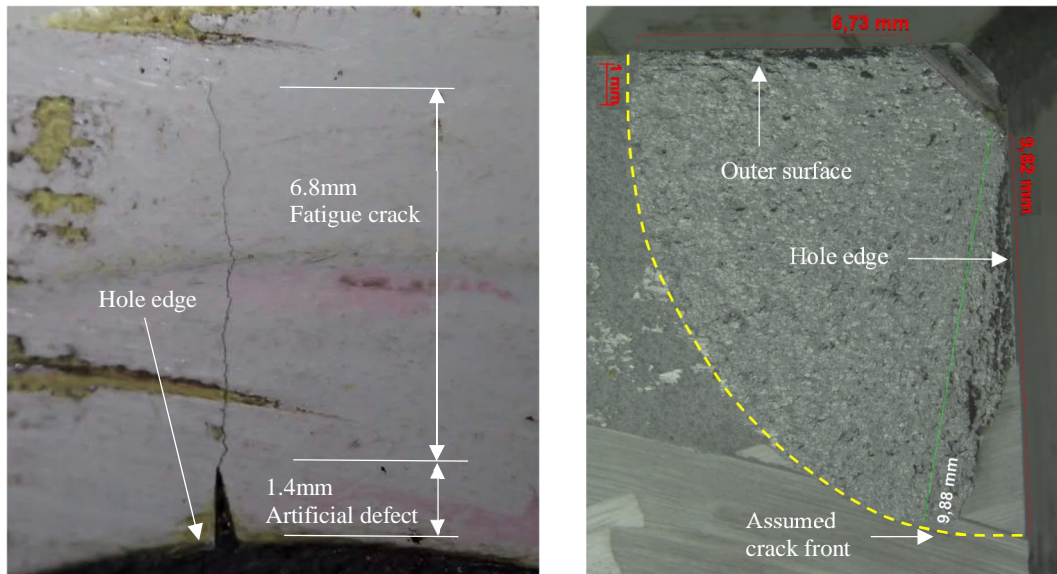


Figure 8: Left: Surface crack at defect #3 at jack attachment lug after 5.75 DL. Image from ref [5]. Right: Opened crack surface. Crack length at outer surface 6.73 mm agrees well with left figure. Unfortunately, the lower right part of the fatigue crack was damaged by sawing during fractography and the crack length at the hole edge is assumed 9.82 mm. Image from ref [6].

ANALYSES

The purpose of the analysis work is to determine the number of 39F DL that the performed test verifies. The evaluation of the verified crack initiation and propagation time for the 39F sequence, based on the tested 39E sequence, is considered as a valid approach because of the similarity of the two sequences. The 39F sequence contains a larger number of load states and slightly larger amplitudes, see Figure 9, but the stress fields for the dominant load cases are similar in both sequences. This has been confirmed by local FE analyses of the stress fields. It can therefore be assumed that both sequences generate the same type of damage in the critical points but after different times. The verified life for sequence 39F is determined as the number of flight hours that gives the same calculated cumulative damage and crack growth as the tested sequence.

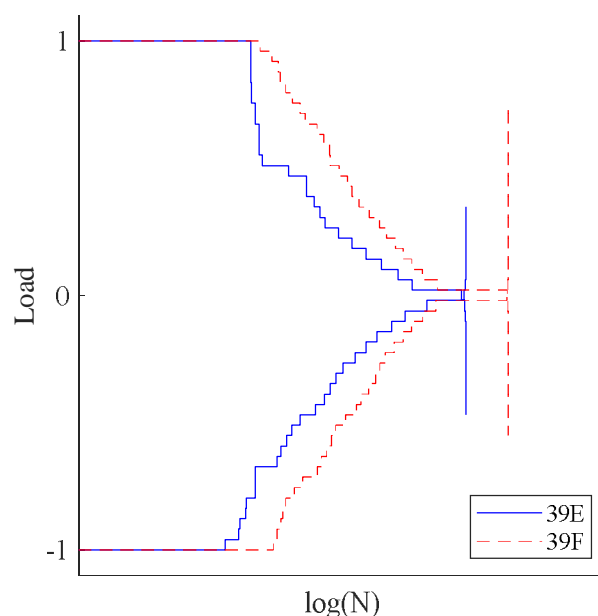


Figure 9: Normalized level exceedance plots of load sequences 39E and 39F.

Although all five critical points were considered in the analysis work, only the critical point at the actuator jack lug, where defect #3 is located, is discussed in this paper. Two types of analyses are performed: a fatigue damage initiation analysis in the lug, based on the method in [7], and a crack growth analysis using Saab in-house method for lugs [8]. Geometry functions for tapered lugs with various load directions and crack positions are calculated using Saab in-house FE-based method [9].

Fatigue damage initiation analysis

The calculation method [7] uses Haigh-diagrams based on constant amplitude tests of longitudinally loaded lugs fitted with non-interference pins which were tested to failure. The method takes into account the stress concentration, the size effect, and the fretting corrosion due to the contact between the pin and the hole edge. For obliquely loaded and tapered lugs a stress concentration correction factor is applied. For variable amplitude loading, the calculation of damage is based on the rain-flow counted cycles and linear Palmgren-Miner cumulative damage assumption. In sizing situations, scatter factors are normally applied to cover the variability associated with fatigue life. However, in the current analysis mean values are used. Figure 10 shows the calculated cumulative damage as function of DL for the 39F sequence and for the tested sequence.

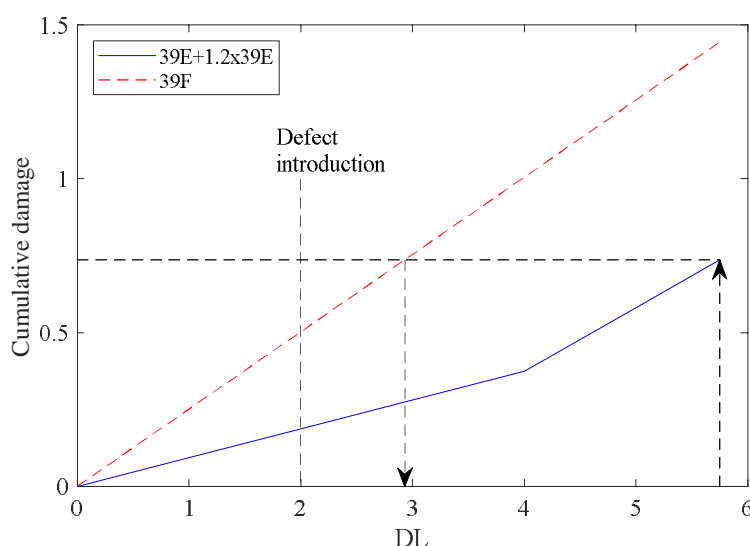


Figure 10: Calculated cumulative damage for 39F sequence and for the test sequence (39E+1.2x39E) at the actuator jack lug.

At the end of the test, 5.75 DL, the calculated damage for the test sequence is 0.74. This damage corresponds to 2.9 DL for the 39F sequence, which verifies at least $2.9/4 = 72\%$ of full life, since 4 tested DL are required for verification of full life. The analyses of all other critical points showed higher percentage of verified 39F life.

Crack growth analysis

The method first uses a plane stress FE-model [9], to compute the geometry functions for a through crack in an obliquely loaded lug with a pin, see Figure 11. Two functions are computed, one for a force prescribed in a direction and one for the reversed load direction. The geometry functions are then corrected by a ratio between the solutions for a through crack and a corner crack in a longitudinally loaded lug. This compounded solution is used for integration of the crack growth rate to compute the crack length as function of the number of cycles, as described in [8]. The calculation is run to the critical crack length, i.e. when the stress intensity factor for a prescribed residual strength load equals the fracture toughness. Figure 12 and 13 show the computed surface and through crack lengths as function of tested DL after the introduction of the artificial defects for the 39F sequence and for the tested sequence. The measured surface crack lengths are also plotted in Figure 12 and 13 for comparison.

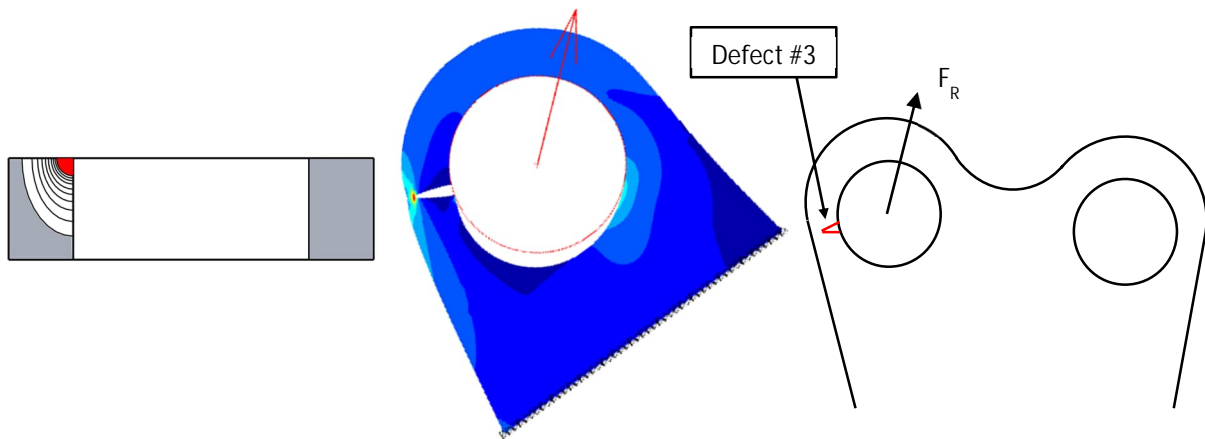


Figure 11: Left: Computed crack contours, Mid: Crack model, Right: Lug geometry.

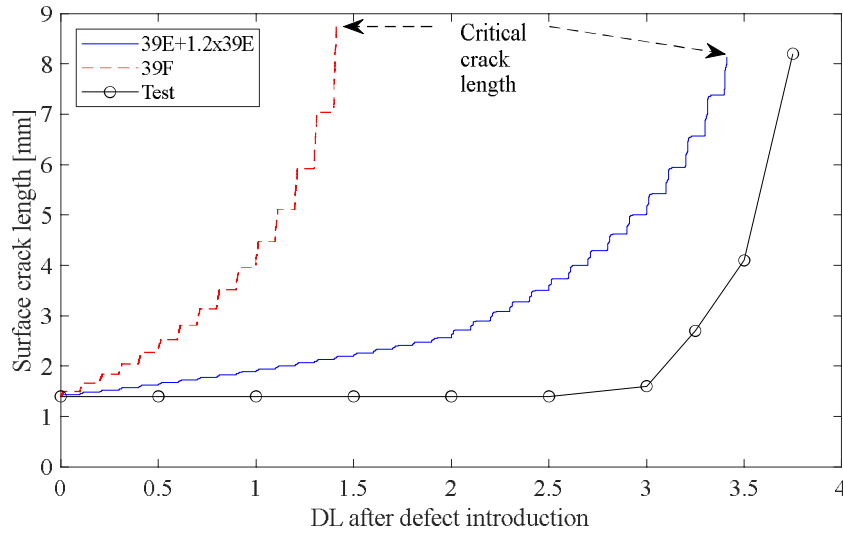


Figure 12: Calculated and measured surface crack length (including the artificial defect length) from defect #3, for the 39F sequence and for the test sequence (39E+1.2x39E).

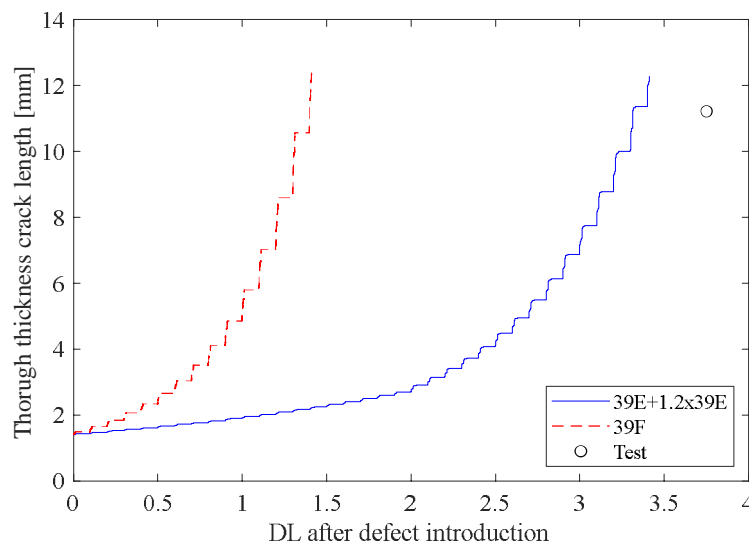


Figure 13: Calculated and measured through thickness crack length (including the artificial defect length) from defect #3, for the 39F sequence and for the test sequence (39E+1.2x39E).

The test was stopped at 5.75 DL, just before the measured crack reached the calculated critical surface length of 8.2 mm at 144% LL. Since the RST at 144% was performed without failure, the calculated critical length can be assumed to be somewhat conservative. The calculated critical length was slightly longer for 39F sequence at was reached at 1.41 DL of 39F sequence, which corresponds to $1.41/2 = 71\%$ of full verified life for DT.

DISCUSSION

The predicted time of crack growth to critical length was 0.34 DL shorter than shown by the test. This discrepancy is partly due to the fact that the fatigue crack in the test did not start to grow immediately after the introduction of the defect. It took around 2 DL of testing until the crack growth was first detected by inspection. However, most of the inspections and crack length measurements were performed with the test object in the rig which may have affected their accuracy. For instance, during the last inspection in the rig, the crack length was measured to be more than 1 millimeter shorter than what was measured during the tear down inspection right after. Due to that reason, it is possible that the crack had started to grow earlier and was in fact longer than measured during the in-rig inspections. In that case, the crack growth rate was lower than the test measurements indicate in Figure 12 and closer to the predicted rate.

The current test and analysis approach has verified full life for 39E sequence and at least 70% of full life with 39F sequence. In light of the fatigue and crack growth analyses, as well as the outcome of the test, it is unlikely that the 39F rudder sequence could have been verified by testing for full service life. Judging by the predicted cumulative damage, and predicted and measured crack growth rate, it is doubtful that 4 DL of safe-life and 2 DL of DT testing could have been reached either with 39F sequence or with continued testing with the 1.2x39E sequence. However, 70% of full life is substantial and is considered as an appropriate time to first in-service inspection.

CONCLUSION

A structural test of Gripen 39E/F rudder was successfully conducted to verify the safe-life and DT of the rudder structure. The test sequence was the 39E sequence, with upscaled loads during a latter part of the test campaign. Thus, the test verified full service life for the 39E sequence. Fatigue and crack growth analyses were performed in order to assess the test results and the amount of verified service life for the 39F sequence was estimated to 70%. Conclusively, the presented procedure showed to be a cost-efficient strategy to utilize the test results, without jeopardizing the primary goal of validating the 39E configuration of the aircraft.

REFERENCES

- [1] Ansell H. (2015). *Structural integrity assessment of Gripen NG aircraft*. In: Proceedings of the 28th ICAF Symposium, Helsinki, Finland.
- [2] Laakso, R., et al. (2022). *Rudder Tests. Customer Report № VTT-CR-00133-20* (classified). VTT Technical Research Centre of Finland Ltd.
- [3] Juntunen, J. and Laakso, R. (2021). *Description of tare procedure. Document № VTT-M-00873-21* (classified). VTT Technical Research Centre of Finland Ltd.
- [4] Saab. (2022). 5.4.3. *Gripen E Test Program, Fatigue and Damage Tolerance testing of the Rudder. Plan, Reg. No JS-91557, Rev. 4* (classified). Saab AB.
- [5] Koskinen, T. (2022). *Inspection report. [NDI on table after 5.75 design lives.] Customer Report № VTT-CR-00459-22* (classified). VTT Technical Research Centre of Finland Ltd.
- [6] Bengtsson A. (2023). *Examination of Defects in Rudder Jack Actuator Lug, test 5.4.3, Test Report PRO23-0956*, Element.

- [7] Larsson S.E. (1969). *The development of a calculation method for the fatigue strength of lugs and a study of test results for lugs of aluminium*. In: Proceedings of the 4th ICAF Symposium.
- [8] Ansell H. (2017). *A review of aeronautical fatigue investigations in Sweden during the period April 2015 to March 2017*. In: Proceedings of the 35th ICAF Conference, Nagoya, Japan.
- [9] Kapidžić Z. (2021). *A review of aeronautical fatigue investigations in Sweden during the period April 2019 to March 2021*. In: Proceedings of the 37th ICAF Conference.